WELDING RESEARCH

SUPPLEMENT TO THE *WELDING JOURNAL*, SEPTEMBER 1987

Sponsored by the American Welding Society and the Welding Research Council

Investigation of Heat-Affected Zone Cracking of GMA Welds of Al-Mg-Si Alloys Using the Varestraint Test

Filler metal composition, rather than base metal composition, promoted or prevented the occurrence of transverse cracking

BY H. W. KERR AND M. KATOH

ABSTRACT. Al-Mg-Si alloys are superior to other high-strength aluminum alloys in their weldability and corrosion resistance, but have a problem of high crack sensitivity in the weld heat-affected zone (HAZ) due to liquation cracking. Some reports have been published on liquation cracking of these alloys. However, there is some disagreement in previous papers over the mechanisms of liquation cracking. In this present investigation, the effects of the filler metals and welding conditions on HAZ cracking were studied for GMA welds of Al-Mg-Si alloys, using the Varestraint test for 4043 and 5356 filler metals. The sensitivity of HAZ liquation cracking was mainly evaluated by the maximum crack length in the HAZ.

Two types of cracking were observed: longitudinal cracking, parallel to the weld bead, and transverse cracking, normal to the weld bead. The longitudinal cracks were observed only in the case of 5356 filler metal. For the longitudinal cracks to be developed, it is necessary that the region near the fusion boundary is melted (probably due to constitutional liquation) and that the weld metal has partly solidified when the augmented strain is applied. The heat input must exceed a critical value in order to cause longitudinal cracking.

The transverse cracks were observed for both 4043 and 5356 filler metals. Both the augmented strain and the heat input must exceed critical values in order to cause transverse cracking. At a given augmented strain and heat input, the maximum crack length was considerably greater in the case of 4043 filler metal than in the case of 5356 filler metal. This phenomenon could be explained by assuming that the lower solidus temperature of 4043 filler metal promoted liquid penetration to the HAZ for a longer distance. A thin layer with higher Si in the case of 4043 filler metal and Mg in the case of 5356 filler metal was observed on the crack surface, consistent with penetration of the molten metal from the weld metal.

The relative cracking tendency is opposite for the two types of cracks with the different filler metals; 4043 filler metal promotes transverse cracking, but prevents longitudinal cracking.

KEY WORDS

GMA Al-Mg-Si Welds
HAZ Liquation Cracks
Crack Mechanisms
Longitudinal Cracks
4043 Al Filler Metal
5356 Al Filler Metal
Varestraint Testing
Heat Input Effects
Solidus Temperature
Transverse Cracking

H. W. KERR is with the Department of Mechanical Engineering, University of Waterloo, Waterloo, Ontario, Canada. M. KATOH is with the Department of Metallurgical Engineering, Kyushu Institute of Technology, Kitakyushu, Japan.

Table 1—Chemical Compositions of Materials Used (wt-%)

	Cu	Fe	Mg	Mn	Si	Ti	Zn	Cr	V	Zr
Commercial 6061	0.25	0.29	0.76	0.044	0.51	0.025	0.080	0.16	0.011	–
Alloy 3 (6261)	0.25	0.20	0.58	0.28	0.82	0.012	–	0.001	0.01	0.001
Alloy 10 (6261)	0.24	0.22	0.58	0.17	0.81	0.013	–	0.001	0.18	0.001
Alloy 17 (6061)	0.99	0.25	1.03	0.015	0.64	0.010	–	0.12	0.009	0.01
Alloy 22 (6061)	0.24	0.20	1.0	0.002	0.57	0.012	–	0.11	0.009	0.001
Alloy 24 (6061)	0.01	0.20	1.01	0.002	0.57	0.011	–	0.11	0.009	0.001
Alloy 25 (6351)	0.23	0.21	0.57	0.02	0.98	0.011	–	0.11	0.01	0.001
4043 filler metal	0.19	0.21	0.018	0.003	4.35	0.10	<0.0003	0.0007	0.016	–
5356 filler metal	0.009	0.25	4.73	0.071	0.077	0.083	0.004	0.070	0.015	–

Introduction

Al-Mg, Al-Mg-Si and Al-Zn-Mg alloys have been widely used as materials for welded structures. Al-Mg alloys are non-heat-treatable, but both Al-Mg-Si and Al-Zn-Mg alloys are heat-treatable. It is said that Al-Mg-Si alloys are superior in their weldability and corrosion resistance, but slightly inferior in strength, to Al-Zn-Mg alloys when Al-Mg or Al-Si filler metals are used (Ref. 1).

However, Al-Mg-Si alloys have a problem of high crack sensitivity in the weld HAZ due to liquation cracking. Some reports have been published on liquation cracking of these alloys. Gittos and Scott showed that HAZ cracking occurred parallel to the weld bead in GMA (gas metal arc) welds, using a patch test (Ref. 2). They attributed cracking to the base metal solidus being below the weld metal solidus. However, Tsujimoto, *et al.*, who performed GMA groove welding in a butt joint, showed that liquation cracking occurs even when the solidus of the base metal is higher than that of the weld metal (Ref. 1). The reason for liquation cracking was considered to be the invasion (or the diffusion) of Si and Mg, which are the major elements of the filler metals, along the grain boundaries of the HAZ (Ref. 1). Tanaka, *et al.*, showed that the HAZ crack sensitivity could be evaluated by the width of the brittle temperature range, defined as the difference in nil-ductility temperatures on heating versus on cooling (Ref. 3).

In a related paper, the authors have shown that HAZ liquation cracking normal to the weld bead occurred in Al-Mg-Si alloys which were GTA welded using the Varestraint test (Ref. 4). It was made clear that cracking only occurred when both the augmented strain and the heat input were above critical values. Moreover, the maximum crack length increased when either the augmented strain or the heat input increased.

It is apparent that there is some disagreement in previous papers over the mechanisms of liquation cracking. Part of the difficulty in interpreting these results is that different testing techniques were used. In addition, the comparison of cracking using different filler metals or welding conditions has generally been qualitative.

In this present investigation, the effects of the filler metals and welding conditions on HAZ cracking were studied for GMA welds, using the Varestraint test. Different compositions of base metals were employed, based on 6061-type alloys. Depending on the sectioning technique, two major types of cracking were observed, each of which could be affected by the welding procedure.

Materials Used and Experimental Procedures

Table 1 shows the chemical compositions of the materials used (thickness: 6.3 mm/0.25 in., length: 120 mm/4.7 in.). Type 6061 alloys, nominally Al-1 Mg-0.6 Si, are balanced Mg_2Si alloys, but may have variations in the contents of Cu, Mn, Cr, V and Zr (commercial 6061 alloy, Alloys 17, 22 and 24). Type 6351 alloys are high in excess Si alloys (Alloy 25), while 6261 alloys have somewhat less excess Si (Alloys 3 and 10). Minor elements such as Cu, Mn, Cr, Zr and V can affect recrystallization and grain growth in the HAZ, as well as precipitation and liquation effects.

The Varestraint test was performed to evaluate the sensitivity of the HAZ liquation cracking. Figure 1 shows a schematic representation of the Varestraint test. GMA welding on plates was performed using welding speeds (v) ranging from 254 to 508 mm/min (10 to 20 ipm), welding currents (I) from 110 to 170 A, and arc voltages (E) from 22 to 24 V. The filler metals used were 4043 and 5356 (diameter 1.6 mm/$\frac{1}{16}$ in.). The specimen was bent approximately one second before the arc for the welding was stopped.

The HAZ liquation cracks were normal and/or parallel to the weld bead, as will

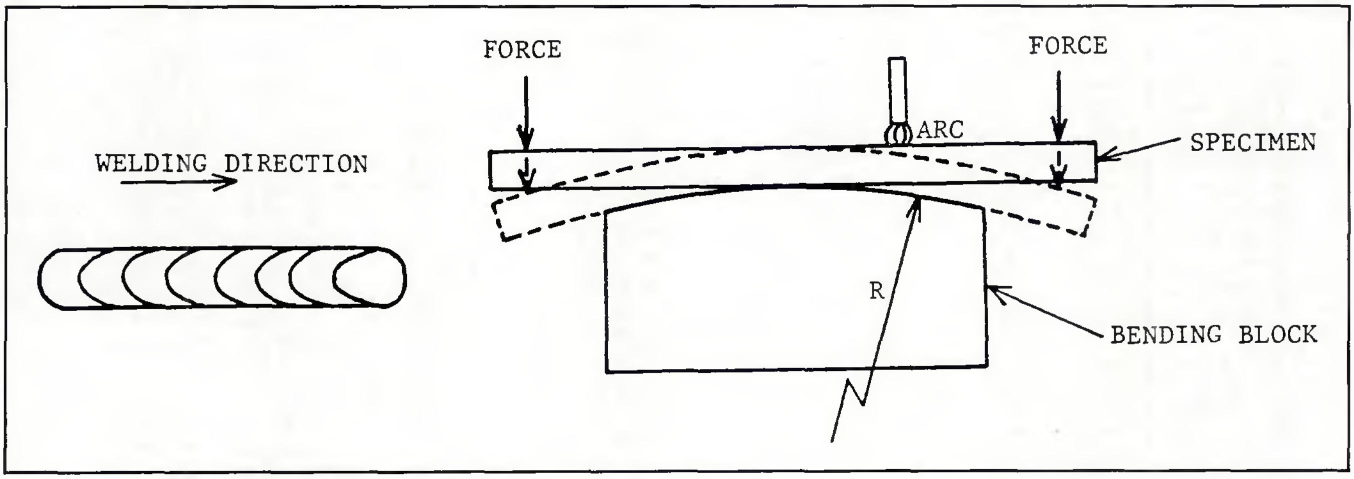

Fig. 1—Schematic representation of the Varestraint test. Left—top view; right—side view

be described in detail later. The radii of the bending blocks were 200 and 100 mm (8 and 4 in.). It was possible to change the bending radii of the specimens by changing the stroke of the equipment.

The sensitivity of the materials to the HAZ liquation cracking was mainly evaluated by the maximum crack length in the HAZ. The crack length was observed using a projector (×20) after machining off the reinforcement. The maximum crack length (L_{max}) changes when either the width of the specimen or the ram speed of the cylinder for bending the specimen is changed (Ref. 4). In this investigation, the width of the specimen was 50 mm (2 in.) and the ram speed was 12.3 mm/s (0.5 ips) (measured in bending the base metal without welding).

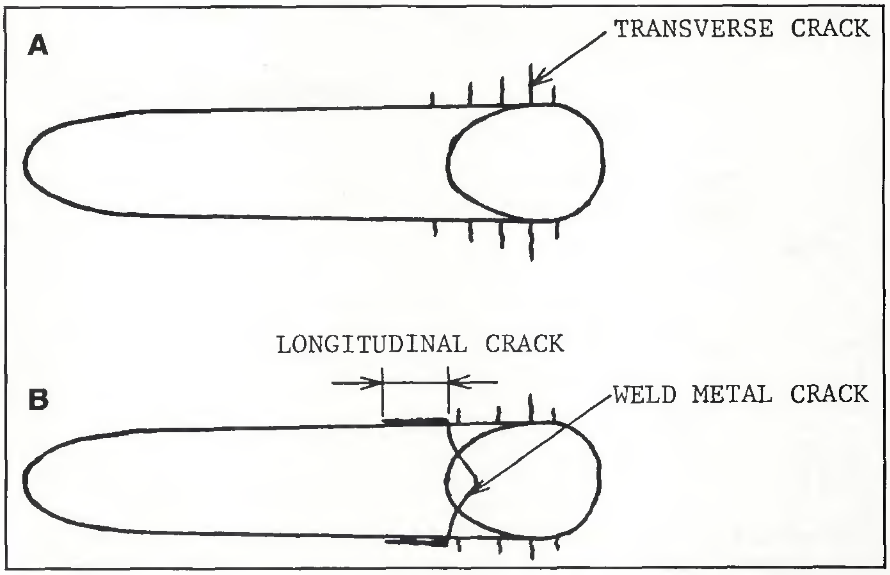

Fig. 2—Schematic representation of cracks observed. A—4043 filler metal; B—5356 filler metal

Crack Types

Figure 2 shows a schematic representation of the cracks observed for the two filler metals, 4043 and 5356. In the case of 4043 filler metal, only cracks which were transverse to the weld bead were observed (these cracks will be called transverse cracks hereafter). The transverse cracks are HAZ liquation cracks. In the case of 5356 filler metal, both transverse cracks and cracks which were parallel to the weld bead (called longitudinal cracks hereafter) were observed.

The longitudinal cracks propagated in the partially molten zone of the HAZ a distance from the weld bead—Fig. 3. In addition, weld metal cracking was observed in the weld crater, following the direction of heat flow, as illustrated in Fig. 2B. This weld metal cracking was not studied extensively in the present investigation, since it was found to be present in all cases, whereas longitudinal cracks were only observed with certain filler metal/weld procedure combinations. Similarly, weld metal cracking was not a necessary condition for transverse cracking of the HAZ, since many transverse cracks were not attached to weld metal cracks.

Longitudinal Cracks

Effects of Augmented Strain and Heat Input

Figure 3 shows a macrostructure of the longitudinal crack. In the cross-section, the crack is observed to be parallel to the fusion boundary. Figure 4 shows a microstructure near the crack. It is clear that the crack is propagating in the partially molten zone.

Figure 5 shows the relation between the crack length and the augmented strain in the case of heat input (Q) equal to 8.3 kJ/cm (21 kJ/in.) (assuming Q = 60 EI/v) for the commercial 6061 alloy. The crack length was measured in the longitudinal section near the fusion boundary. The augmented strain ϵ was obtained using Equation 1:

$$\epsilon = t/2R \quad (1)$$

where t is the thickness of the specimen (6.3 mm) and R is the radius of the bending (mm). As the weld metal has a reinforcement, the strain in the weld metal cannot be given by Equation 1. The strain shown here is the value on the specimen surface without the reinforcement. The crack length increased gradually when the augmented strain increased. As will be shown later, there was a critical augmented strain to cause the transverse cracks. In the case of the longitudinal cracks, however, a longitudinal crack about 4 mm (0.15 in.) long was observed even when the augmented strain was small, down to 0.6%.

Figure 6 shows the relation between the longitudinal crack length and the heat input in the case of augmented strain equal to 3.2%. For heat inputs less than 4.3 kJ/cm (11 kJ/in.), no longitudinal cracks were observed. When the heat input was larger than 4.3 kJ/cm, the crack length increased linearly with heat input.

Figure 7 shows fractographs of the fracture surface of the commercial 6061 alloy's longitudinal crack. Figure 7A is opposite the weld crater, but in the HAZ. Evidence of a solidification structure is visible, showing that the fracture surface was melted when the longitudinal crack was developed. Figure 7B is a region a

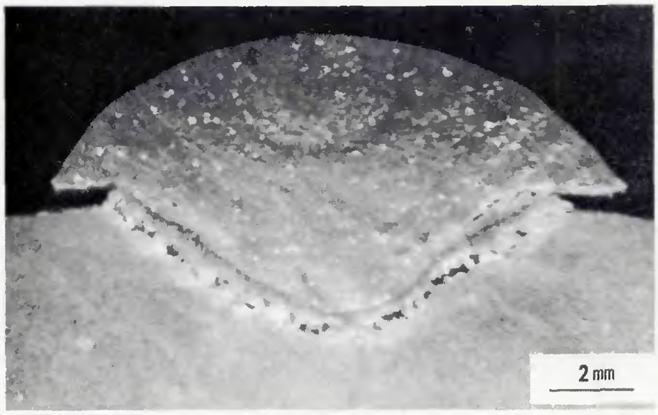

Fig. 3—Macrostructure of a longitudinal crack

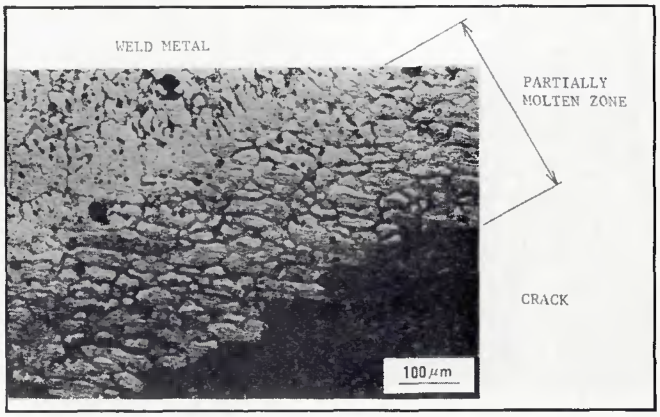

Fig. 4—An example of microstructures near the longitudinal crack

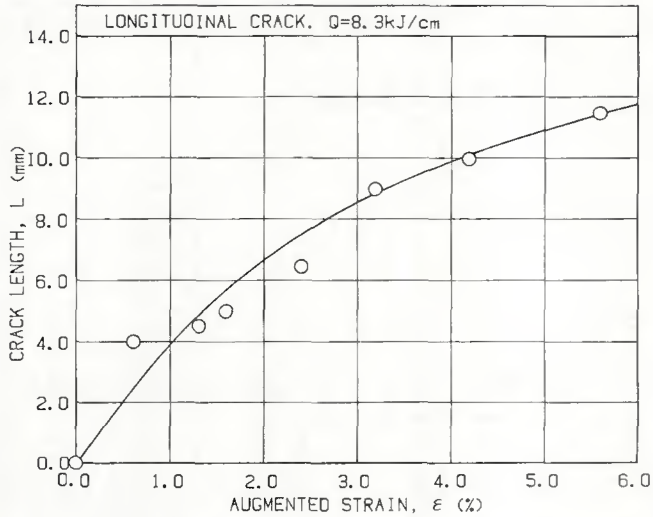

Fig. 5—Relationship between the crack length of the longitudinal crack and the augmented strain

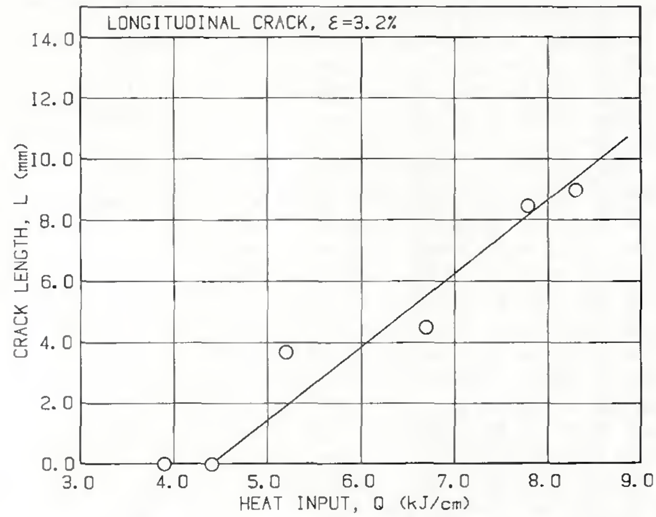

Fig. 6—Relationship between the crack length of the longitudinal crack and the heat input

little farther behind the crater; solidification structure is still visible. Analysis of the globular shapes, using an energy dispersive x-ray analyzer (EDX) on a scanning electron microscope, indicated that they are compounds, with a range of compositions: 2 to 7 wt-% Mg, 5 to 9 wt-% Si, 7 to 19 wt-% Fe and 1 to 2 wt-% Cu. The numbers of the compounds decrease when the distance from the crater increases, as is seen in Fig. 7C. Because of the small size of the compounds, these analyses will be affected by the surrounding matrix. However, the high percentages of alloying additions, particularly Fe, are very noteworthy. It is clear that these compounds are due to liquation, but not certain whether the higher content of Mg is due to diffusion and/or invasion from the weld metal, or simply melting of the existing element in the base metal. Figure 7D is near the end of the crack. In this case, the grain boundary is sharper than the other fractographs. These fractographs show that the amount of molten metal decreases when the distance from the crater increases.

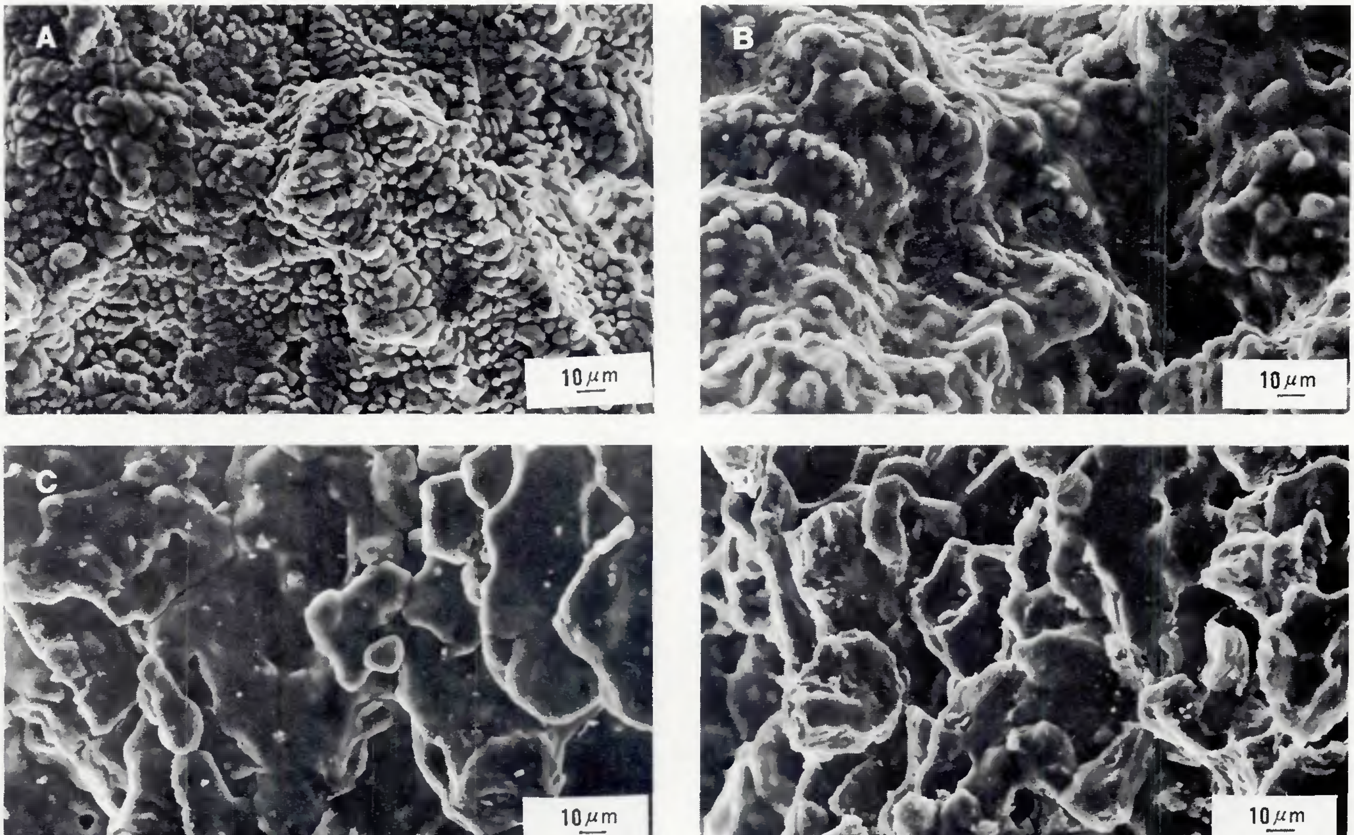

Fig. 7—Examples of fractographs of the longitudinal crack. A—near the weld crater; B—a little farther from the weld crater; C—far from the weld crater; D—near the end of the crack

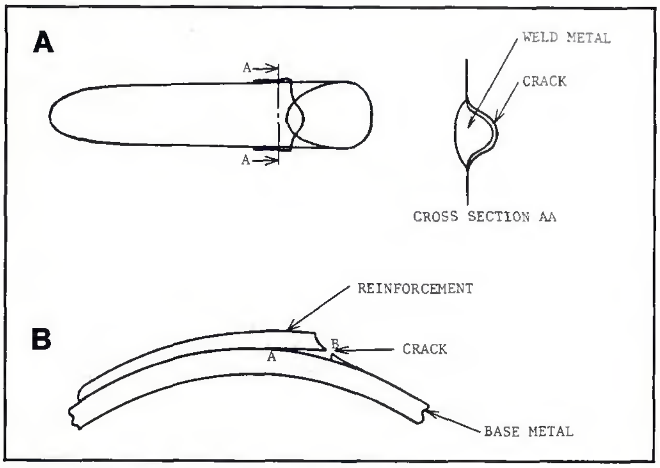

Fig. 8 — A — Top and B — side views of the longitudinal crack

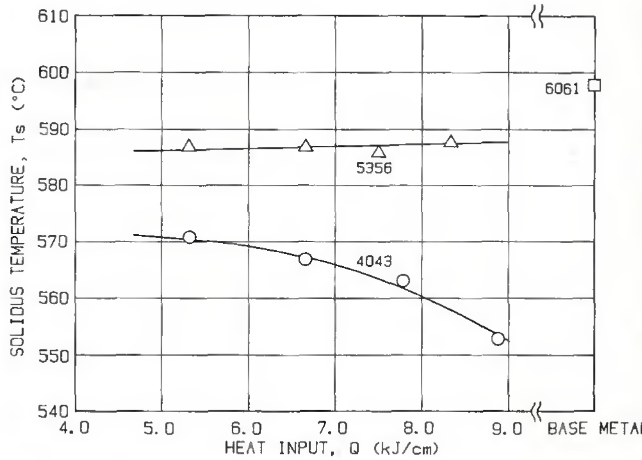

Fig. 9 — Relationship between the solidus temperature (using DSC) and the heat input

Mechanism of Longitudinal Cracking

Figure 8 shows the top and side views of the longitudinal crack. As seen in the side view, the reinforcement bent where there was no crack, but bent less near the region where the crack was observed. This shows that the weld metal on top of the crack was largely solid when the augmented strain was applied. It is clear from Fig. 7 that the fracture surface is melted, with increasing liquid closer to the weld crater. Hence, for the longitudinal crack to be developed, it is necessary that the region near the fusion boundary is melted and that the weld metal has partly solidified when the augmented strain is applied.

Gittos and Scott estimated the relation between the solidus temperature and dilution by the base metal, using the Al-Mg-Si ternary phase diagram (Ref. 2). They proposed that, during welding, grain boundary melting occurs in the HAZ, and that with certain base metal and weld metal compositions, it is possible for the base metal solidus to be below the weld metal solidus. Thus, when tensile strains arising from weld metal solidification are imposed on the HAZ, longitudinal cracking occurs at such boundaries.

To examine this theory, the solidus temperatures of the weld metals and the base metal were measured using a differential scanning calorimeter (DSC). Figure 9 shows the relation between the solidus temperatures and the heat input for the two filler metals. In the case of 4043 filler metal, the solidus temperatures were much lower than those of the base metal (598°C/1108°F) because of dilution, and decreased from 571° to 553°C (1060° to 1027°F) as the heat input increased from 4.4 to 8.9 kJ/cm (11 to 23 kJ/in.). Consistent with Gittos and Scott, no longitudinal crack was observed using this filler metal. In the case of 5356 filler metal, the solidus temperature increased slightly, from 585° to 588°C (1085° to 1090°F), as the heat input was increased from 4.4 to 8.3 kJ/cm, but was still a little lower than that measured for the base metal (598°C). Hence, the cracking observed in this case is not consistent with the Gittos and Scott mechanism.

Pepe and Savage have shown that the HAZ may liquate due to constitutional liquation (Ref. 5). This appears to be the mechanism for the longitudinal cracking in the case of 5356 filler metal. The important role played by the minor impurity iron should not be ignored since high values of iron were found in the globular phases. More work is needed on the complex phase equilibria in Al-Mg-Si-Cu-Fe-X alloys (Ref. 6).

When the HAZ can liquate, the reason the longitudinal crack is observed behind the weld crater as shown in Fig. 8A can be explained using Fig. 10. Figure 10A identifies two cross-sections. Cross-section AA ahead of the weld shows an area where no longitudinal crack is observed, while BB shows an area where the crack is observed. Figure 10B shows some locations in the cross-section — Z1 is the weld metal near the fusion boundary, Z2 is the HAZ near the fusion boundary (partially molten zone), and Z3 is the HAZ far from the fusion boundary. Figure 10C shows the thermal cycles at the locations of Z1, Z2 and Z3. Figure 10D shows the temperature distribution in the cross-section AA and corresponds to the temperatures at the time t1 in Fig. 10C. Figure 10E shows the temperature distribution in the cross-section BB and corresponds to the temperatures at the time t2 in Fig. 10C.

Consider that the solidus temperature of the weld metal is higher than the solidus temperature of the base metal. This corresponds to the situation that the HAZ liquates, as in the case of 5356 filler metal. In the cross-section AA, the temperature T1′ at Z1 is the same as that of the molten metal. The temperature T2′ at Z2 is higher than the solidus temperature of the base metal, so there is some liquid at Z2. When the augmented strain is applied, the base metal deforms, but not in the area where there exists enough liquid (that is, both the HAZ partially molten zone and the weld metal). Hence, no longitudinal crack is observed. In the cross-section BB, the temperature T1 at Z1 is lower than the solidus temperature of the weld metal, so that the area near Z1 has already solidified. There exists some liquid near Z2, however, because the temperature T2 at Z2 is higher than the solidus temperature of the base metal. Of course, there is no liquid near Z3. When the augmented strain is applied, the base metal and the HAZ at Z3 deform, but the partially molten zone at Z2 cannot deform without cracking, because the solidified weld metal acts as a restraint. In other circumstances, such as the patch test employed by Gittos and Scott, the base metal is restrained and the partially molten zone cannot deform plastically in response to the cooling of the weld metal.

When the solidus temperature of the weld metal is lower than the solidus temperature of the base metal, as in the case of 4043 filler metal, the weld metal remains partially melted when there is some liquid in the partially molten zone. This is the same case as that in the cross-section AA already mentioned. Hence, no longitudinal crack is observed in this case.

At a given heat input, the amount of liquation decreases as the distance from the weld crater increases. With increased strain, cracking can proceed to a lower fraction of liquid, increasing the crack length as shown in Fig. 5. When the heat input increases, liquation will occur over a wider region. Hence, longer cracks are obtained when the heat input increases at a given augmented strain, as shown in Fig. 6. Heat input above a critical value was necessary to promote the longitudinal cracks, as seen in Fig. 6. At low heat

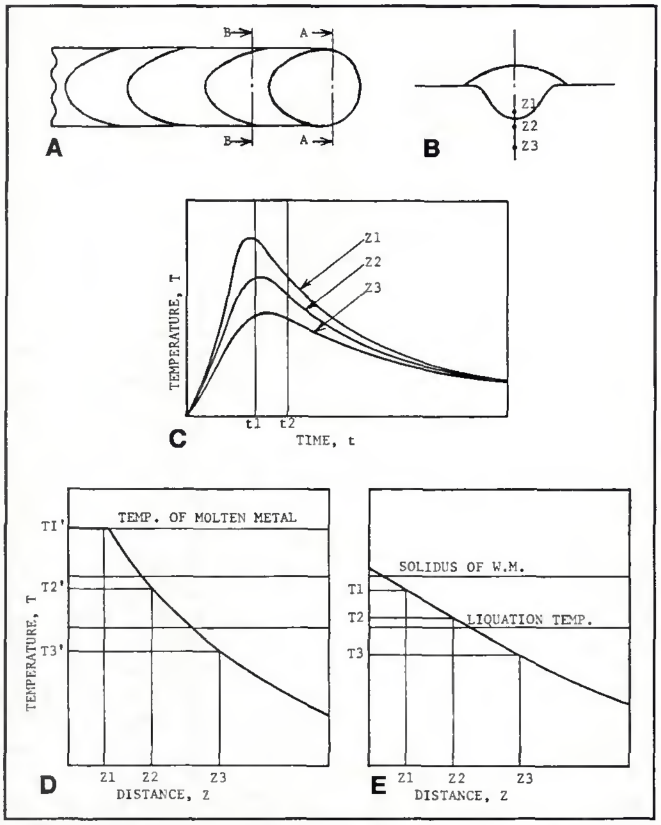

Fig. 10—Schematic representation of the temperature distribution. A—Locations of cross-sections; B—cross-section; C—thermal cycles; D—cross-section AA; E—cross-section BB

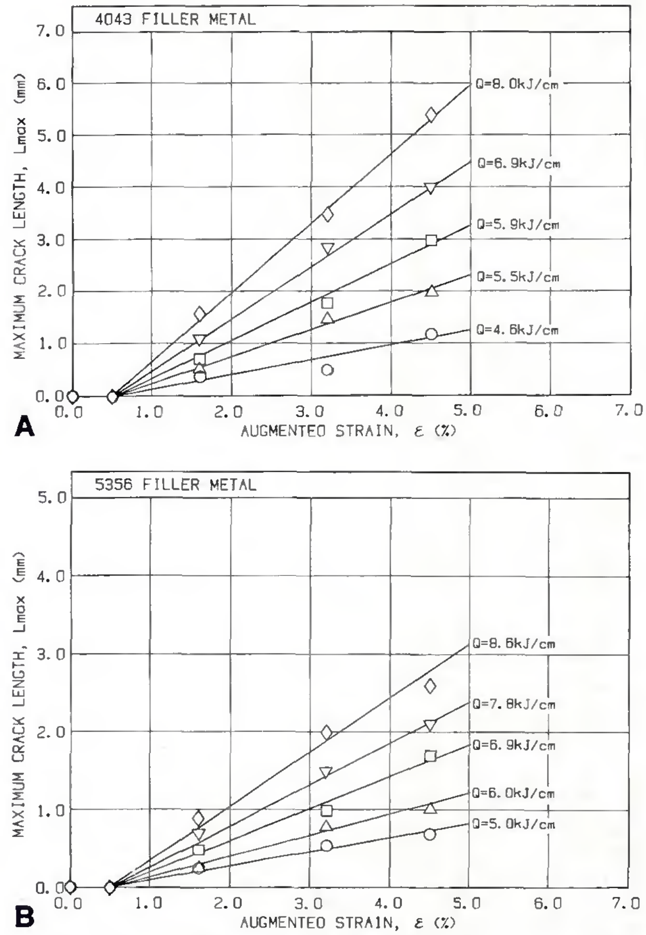

Fig. 11—Relationship between the maximum crack length and the augmented strain. A—4043 filler metal; B—5356 filler metal

inputs, the thickness of the partially molten zone is less than the grain size of the HAZ, so that solid metal is always present to transmit the imposed strain.

Transverse Cracks

Effects of Augmented Strain, Heat Input and Filler Metals

Figures 11A and B show the relation between the maximum transverse crack length and the augmented strain for 4043 and 5356 filler metals, respectively, when using the commercial 6061 alloy. No transverse cracks were observed when the augmented strain was less than about 0.5% for both filler metals. The maximum crack length increased linearly as the strain increased above about 0.5%. At a given augmented strain, the maximum crack length became longer when the heat input was increased.

Figures 12A and B show the relation between the maximum crack length and the heat input for the filler metals 4043 and 5356, respectively. No cracks were observed when the heat input was less than about 4 kJ/cm (10 kJ/in.). When the heat input became larger than 4 kJ/cm, the maximum crack length increased linearly with heat input.

Hence, it is clear that critical values of both the augmented strain and the heat

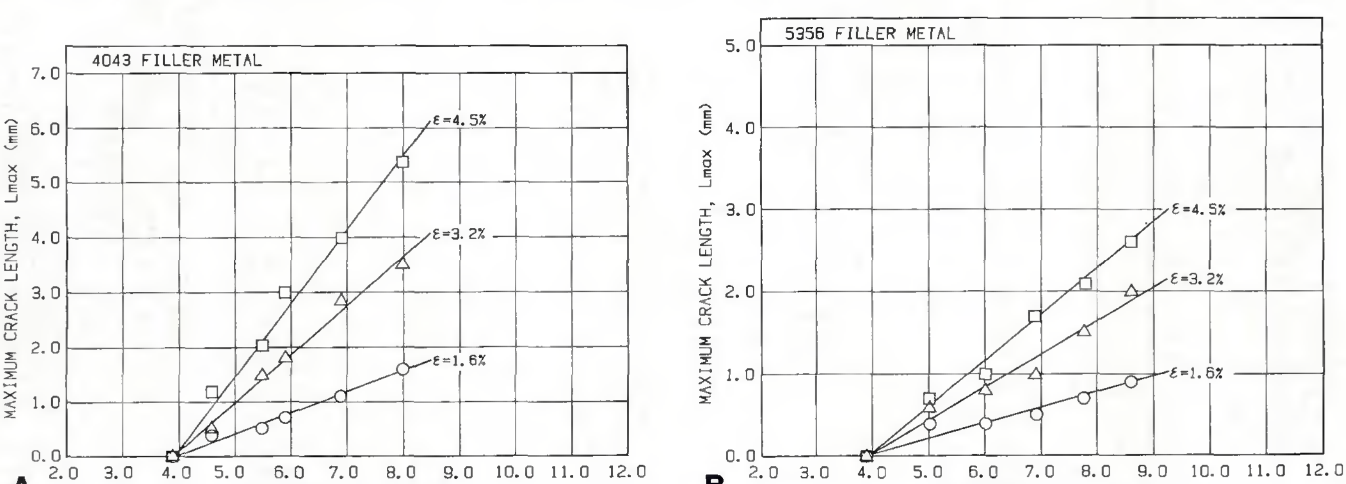

Fig. 12—Relation between the maximum crack length and the heat input. A—4043 filler metal; B—5356 filler metal

input must be exceeded to cause transverse cracking.

The filler metal also considerably influences transverse cracking. Comparing Fig. 12A with Fig. 12B, the maximum crack length in 4043 filler metal was generally more than twice that in 5356 filler metal for a given test condition.

It should be noted that the relative cracking tendency is opposite for the two types of cracks with the different filler metals — 4043 filler metal promotes transverse cracking, but prevents longitudinal cracking.

Figure 13 shows the effect of different base metals on the relationship between the maximum crack length and the heat input, for a fixed augmented strain of 4.5%. The maximum crack length using 4043 filler metal was up to 2.4 times longer than in the case of 5356 filler metal, though the scattering of the data was large. This tendency was the same as that shown in Fig. 12, although the transverse cracks were smallest in the case of the commercial 6061 alloy, as is seen in Fig. 13. It was observed that the effect of the filler metals was larger than that of the base metals.

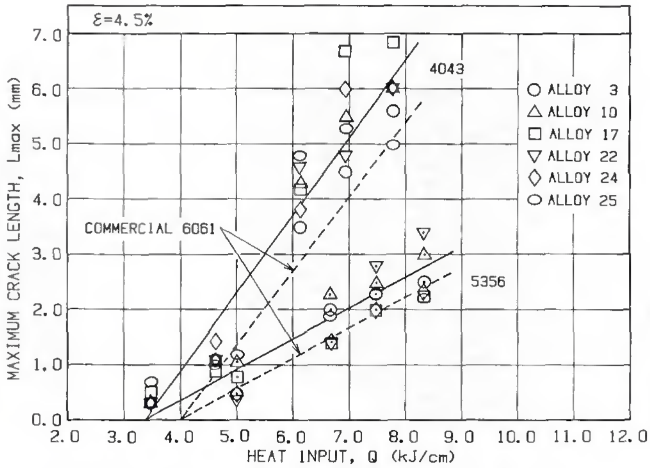

Fig. 13 — Effect of the base metals on the relationship between the maximum crack length and the heat input

Mechanism of Transverse Cracking

Figures 14A through D show fractographs of the transverse cracks in commercial 6061 in the case of 4043 filler metal. Figure 14A is a fractograph from near the fusion boundary. Figures 14B, C and D are fractographs from the locations of y ≈ 30, 70 and 100% in the HAZ, respectively (y = 0% represents the fusion boundary, and y = 100% represents the boundary between the transverse crack and the subsequent crack propagation [by ductile fracture] at room temperature in order to expose the crack surface). Many globular structures are observed in Figs. 14A, B and C, and the numbers of the globular structures decrease as y increases. According to the EDX analysis, these globs contained about 10 to 20% Si. Laminated structures due to the rolling pattern are observed in the upper part of Fig. 14D.

Figures 15A, B and C show fractographs at the locations of y ≈ 0, 50 and 100%, respectively, for the case of 5356 filler metal of the commercial 6061 alloy. Many globular structures, which contained about 8% Mg according to the EDX analysis, are observed all over the crack.

It is clear from Figs. 14 and 15 that the region where the transverse cracks were observed was partly melted during cracking.

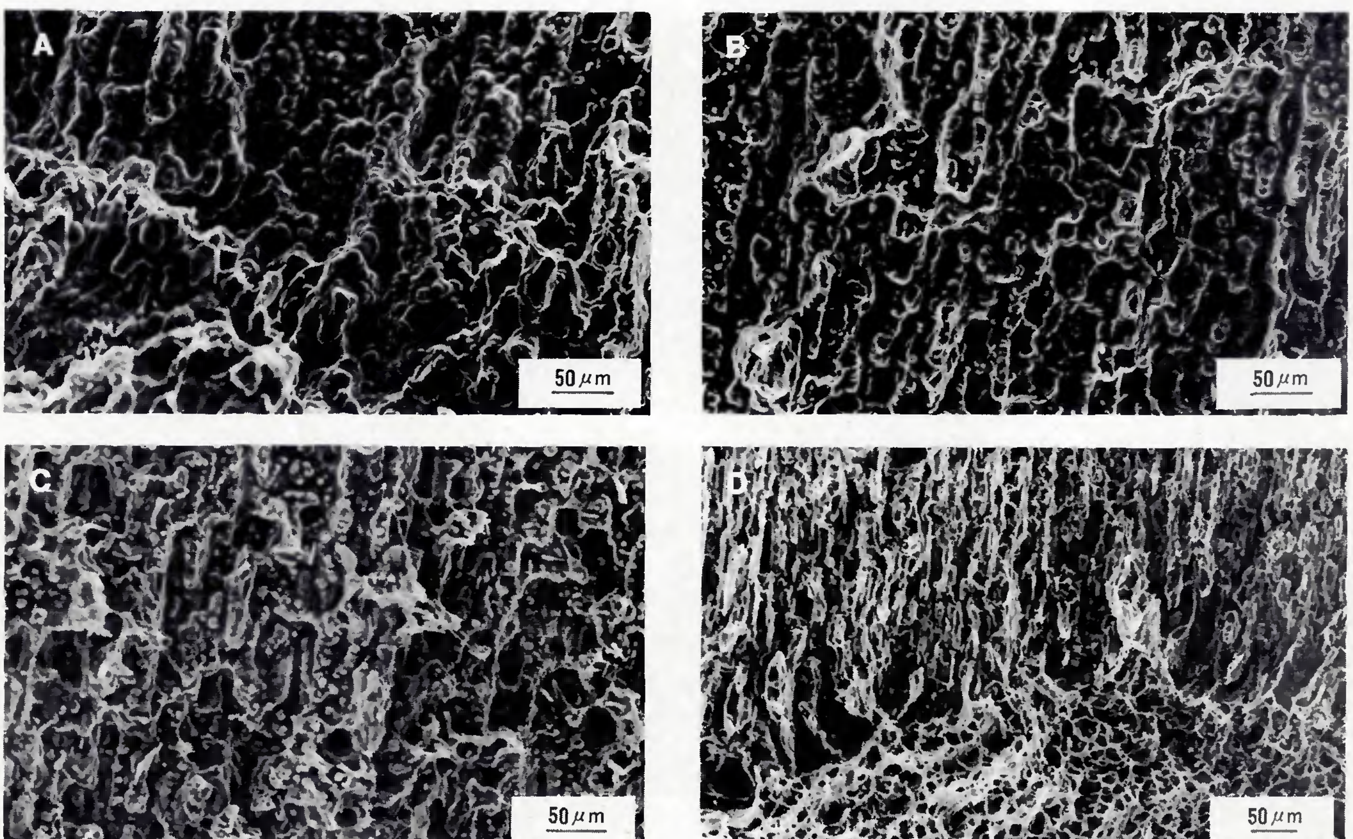

Fig. 14 — Examples of fractographs of the transverse crack (4043 filler metal). A — y ≈ 0% (near the fusion boundary); B — y ≈ 30%; C — y ≈ 70%; D — y ≈ 100% (near the end of the crack)

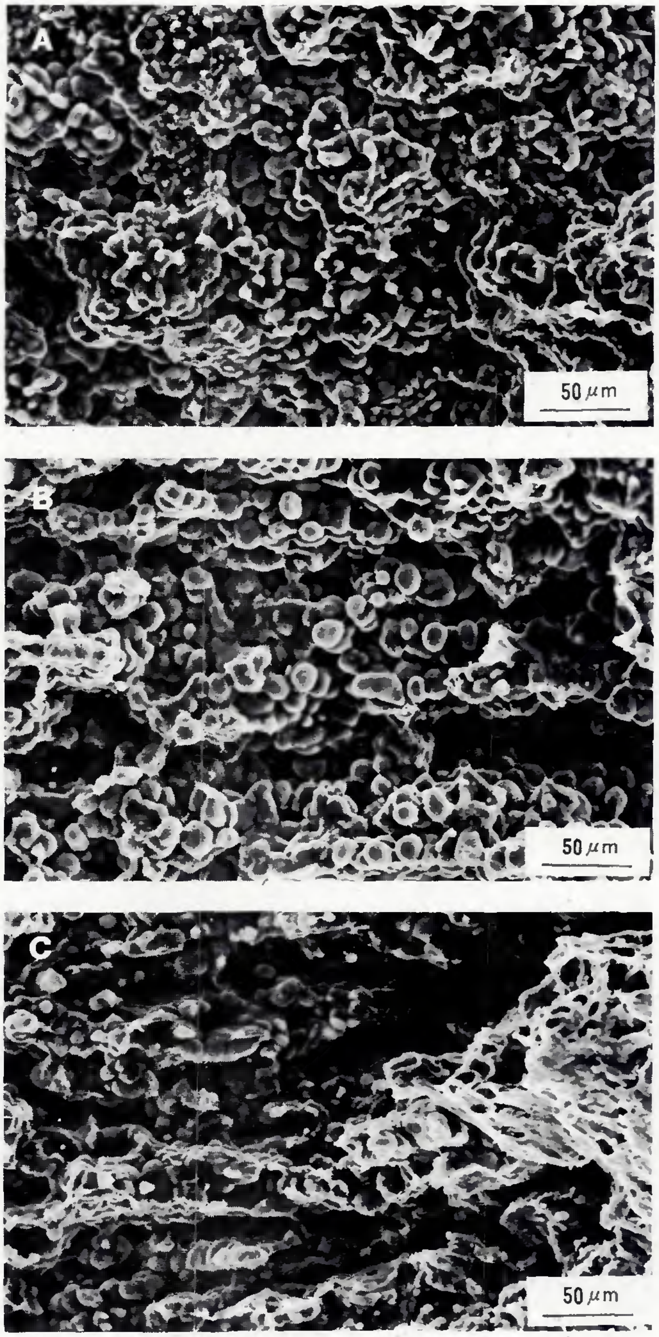

Fig. 15 — Examples of fractographs of the transverse crack (5356 filler metal): A — $y \approx 0\%$ (near the fusion boundary); B — $y \approx 50\%$; C — $y \approx 100\%$ (near the end of the crack)

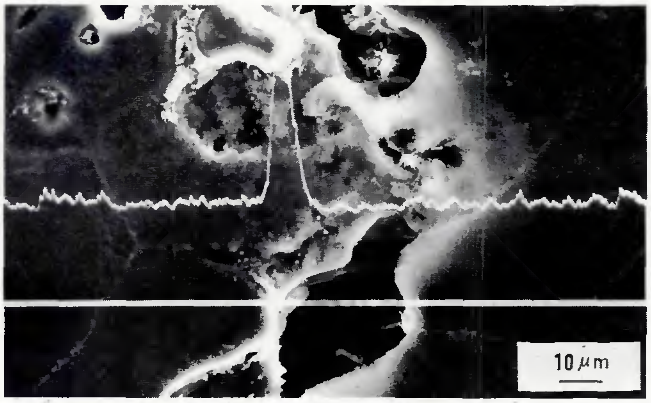

Fig. 16 — The result of line analysis of Si near a crack in the case of 4043 filler metal

Fig. 17 — The result of line analysis of Mg near a crack in the case of 5356 filler metal

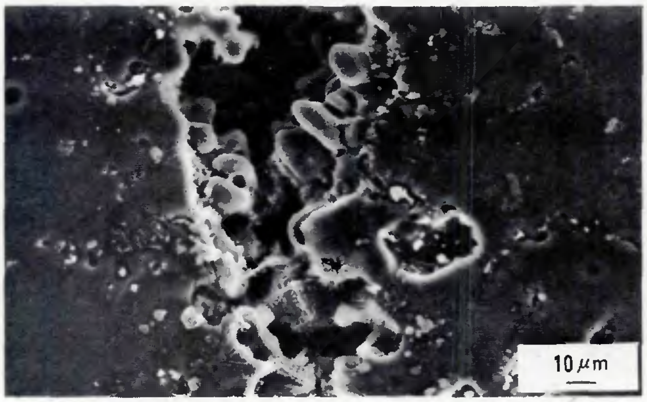

Fig. 18 — An example of microstructures near a crack (5356 filler metal)

Figure 16 shows the result of line analysis of Si near a crack in the case of 4043 filler metal. Figure 17 shows the result of line analysis of Mg near a crack in the case of 5356 filler metal. In each case, a higher content of Si or Mg, respectively, was observed just near the crack. The content of Si or Mg decreased near the end of the crack. This shows that there existed a thin layer rich in Si or Mg on the crack surface.

Different mechanisms have been proposed for liquation in the HAZ, *e.g.*, constitutional liquation (Ref. 5) and low-temperature eutectics due to diffusion or invasion of some elements from the weld metal (Ref. 1).

The observation of higher Si in the case of 4043 and higher Mg in the case of 5356 filler metal is consistent with elements from the filler metals affecting cracking. It is hard to explain the effect of the filler metals on cracking according to constitutional liquation.

The observations are also not consistent with diffusion from the weld metal. The maximum crack length was about 6 mm (0.24 in.) at most. Assuming a diffusion coefficient for the liquid of 10^{-5} cm^2/s and diffusion time of 1 s, the calculated diffusion distance is on the order of 0.03 mm (0.001 in.). Hence, no element could diffuse the distance of up to 6 mm. No marked segregation of Si or Mg was observed at the grain boundaries in the absence of a crack. Therefore, the phenomenon is not consistent with simple diffusion or invasion.

Because the times involved are so

short, it is not possible to actually observe the cracking sequence and liquid movement. The most logical explanation for transverse cracking is the influence of molten metal penetrating from the weld metal along grain boundaries in the partially molten zone. The penetration of liquid will be affected by the surface energy and the liquid fluidity. In general, aluminum liquids which are richer in silicon are thought to be more fluid, implying that penetration should be easier for 4043 than for 5356 filler metal, as observed.

If the cracking is aided by penetration of liquid from the weld metal, the detrimental effects of 4043 filler metal appear to be explained. First, the lower solidus temperatures with 4043 filler metal permit liquid to be present to a lower temperature, thus promoting cracking. Secondly, increased fluidity of Al-Si alloys would aid such liquid penetration. The further application of strain eventually opens a crack at certain grain boundaries, and after that, liquid films on the crack surfaces solidify. The evidence of the solidification of the liquid towards the center of the crack is clearly observed in Fig. 18. When the heat input rises, the region of the HAZ above the solidus temperature of the weld metal increases, thus increasing the maximum crack length.

The proposed process of transverse cracking is as follows: 1) a partially molten zone is developed by welding, whose width widens with increased heat input; 2) augmented strain above a critical value is applied; 3) molten metal from the weld metal penetrates into the grain boundaries, promoting cracking; and 4) the liquid film on the crack surface solidifies.

Hence, the development of the transverse cracks can be explained by the phenomenon of penetration of the molten metal. The relative effects of the two filler metals on the maximum crack lengths can be explained using the difference of the solidus temperatures of the weld metals, but may also be influenced by fluidity effects.

Summary and Conclusions

An investigation was made of the effects of filler metals, heat input and augmented strain on liquation cracking in the HAZ of Al-Mg-Si alloys which were GMA welded, using the Varestraint test. The conclusions obtained are as follows:

1) Two types of cracking were observed — longitudinal cracking, parallel to the weld bead, and transverse cracking, normal to the weld bead. The longitudinal cracks were observed only in the case of 5356 filler metal, but not when 4043 filler metal was used.

2) For the longitudinal cracks to be developed, it is necessary that the region near the fusion boundary is melted (probably due to constitutional liquation) and that the weld metal has partly solidified when the augmented strain is applied.

3) The heat input must exceed a critical value in order to cause longitudinal cracking. At higher heat inputs, the crack length increased linearly with increased heat input.

4) The transverse cracks were observed for both 4043 and 5356 filler metals.

5) A thin layer with higher Si in the case of 4043 filler metal and Mg in the case of 5356 filler metal was observed on the crack surface of the transverse cracks, consistent with penetration of molten metal from the weld metal.

6) Both the augmented strain and the heat input must exceed critical values in order to cause transverse cracking. At a given augmented strain, the maximum crack length increased linearly when the heat input was increased more than the critical value. At a given heat input, the maximum crack length increased linearly when the augmented strain was increased more than the critical value.

7) At a given augmented strain and heat input, the maximum transverse crack length was considerably greater in the case of 4043 filler metal than in the case of 5356 filler metal. This phenomenon could be explained by assuming that lower solidus temperature of 4043 filler metal promoted liquid penetration to the HAZ for a longer distance.

8) The effect of the filler metals on transverse cracking was greater than that of base metal compositions, for a range of experimental plate compositions with varying Si, Mg, Cu, Ti, Cr and V levels.

9) The relative cracking tendency is opposite for the two types of cracks with the different filler metals; 4043 filler metal promotes transverse cracking, but prevents longitudinal cracking.

Acknowledgments

This work was supported by a grant from the Natural Sciences and Engineering Research Council of Canada, and by the University of Waterloo. Alcan graciously supplied the base metals and filler metals, and also carried out the chemical analyses and differential scanning calorimetry. Mr. B. Altshuller of Alcan made useful comments on the work. Messrs. N. Wilhelm, A. Degroot and H. Kamler provided important technical support at the University.

References

1. Tsujimoto, K., Sakaguchi, A., Kinoshita, T., Tamaka, K., and Sasabe, S. 1983. HAZ cracking of Al-Mg-Si alloys. IIW Doc. IX-1273, pp. 1-13.

2. Gittos, N. F., and Scott, M. H. 1981. Heat-affected zone cracking of Al-Mg-Si alloys. *Welding Journal* 60(6):95-s to 103-s.

3. Tanaka, K., Kogane, K., and Yoneda, Y. 1984. Weld heat-affected zone cracking of Al-Mg-Si alloys (part 3). *J. Light Met. Weld.* 22(6):282-289 (in Japanese).

4. Katoh, M., and Kerr, H. W. Investigation of heat-affected zone cracking of GTA welds of Al-Mg-Si alloys using the Varestraint test. To be published.

5. Pepe, J. J., and Savage, W. F. 1967. Effects of constitutional liquation in 18-Ni maraging steel weldments. *Welding Journal* 46(9):411-s to 422-s.

6. Gustafsson, G., Thorvaldsson, T., and Dunlop, G. L. 1986. The influence of Fe and Cr on the microstructure of cast Al-Si-Mg alloys. *Met. Trans.* 17A(1):45-52.